Experiment 6: Franck-Hertz Experiment v1.3

Background


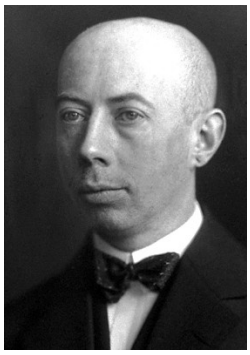

This series of experiments demonstrates the energy quantization of atoms. The concept was first implemented by James Franck and Gustaf Ludwig Hertz in 1914. They showed that an electron must have a specific, well-defined energy to make an inelastic collision with a mercury atom. This energy corresponds to an excited quantum state. In 1926, Franck and Hertz were awarded the Nobel Prize in Physics for conclusively confirming the Bohr model.

There are two parts of this lab. The first experiment is with helium gas and the second uses mercury vapor as was originally done by Franck and Hertz. The essential idea in both measurements is the same. Electrons are injected into an atomic gas at a tunable, precisely defined energy using an electron gun. The energy is set by an adjustable accelerating potential. When incident electrons have energy close to a quantum energy separation in the atoms, they can lose energy efficiently. This happens via inelastic collisions, which reduce the energy of the free electrons by the quantum excitation. The electrons slow down and this is observed as a change in the collector ring current. By recording current as a function of electron kinetic energy (i.e. accelerating voltage), distinct structure can be identified corresponding to quantum energy resonances.

The helium apparatus also allows the observation of ionization. If the energy of the free electrons is made sufficiently large, bound electrons in the helium atom can be liberated. An ionizing collision leaves a positively charged helium ion and two electrons (one incident and one knocked off the atom). Because an additional electron is created at each collision, the conductivity of the gas will increase leading to a corresponding sharp increase of detector current. Both resonant excitation and ionization can be observed with helium.

The experiment is automated using a data acquisition device (DAQ) controlled by a LabView program on a PC. The experimenter must carefully configure acquisition parameters with an understanding of the instrument capabilities and limitations. The block diagram of the LabView program contains its code. This can be inspected if desired, but should not be modified without permission of the instructor.

Part 1: Excitation and ionization of helium

1.1 Equipment

Hertz Critical Potentials tube filled with helium gas
0096 control unit
Pico-amplifier (Note: the detachable digital ammeter display is not used)

Filament power supply (≤ 2.5V at ~ 1 A)
Anode power supply (0—30V)
1.5V battery
PC with LabView program
Digital multimeter

The glass tube houses a cathode ray gun that injects a diverging beam of electrons into low pressure helium gas. Free electrons are created by thermionic emission at a heated tungsten filament. Electrons are accelerated from the cathode towards and past the anode ring into the main volume of the glass bulb. Their kinetic energy is precisely controlled by the anode power supply. A metal ring electrode functions as a collector and is positioned along the perimeter of the bulb so that it does not collect electrons directly from the source beam. Instead, it detects primarily scattered electrons, aided by a small potential from the 1.5 V battery. The ring current flows to a sensitive electrometer through a shielded coaxial cable terminated by a BNC connector. The glass bulb is covered with a thin metallic coating that is at the same potential as the anode, but electrically isolated from the wire ring.

1.2 Objectives

1) Determine energy levels in helium and report their values in units of *eV,* along with estimated uncertainties. Compare to the established values.
2) Determine the ionization energy of helium in *eV* and compare to the known value.
3) Measure the full-width at half-maximum of each peak; determine other sources of error.
4) Study the effect of filament voltage, while keeping it below 2.5V.

1.3 Procedure

Make the electrical connections as shown in Fig. 1. First, wire the filament ports F3 and F4 to a low voltage power supply capable of delivering ~ 1 A. Be sure to observe the indicated polarity. Connect a digital multimeter to the supply to monitor the filament DC voltage. It is important that this voltage does not exceed 2.5V. Turn on the power supply and increase the voltage to > 2V. You should observe current flowing on the power supply ammeter accompanied by an orange glow emanating from the filament inside the tube.

Turn off the filament and connect the DC anode supply (0—30V) to the control unit as shown. If a female banana connector is unavailable, use an alligator clip on connector A1. Be sure to connect C5 to F4.

The 1.5V battery provides a DC bias voltage to collect electrons at the wire ring. When the battery positive terminal is grounded to the amplifier as shown in the figure, the circuit can detect peaks in the current as the anode voltage is varied. These peaks correspond to energy resonances in helium.

Reversing the polarity will attract positive charges instead of negatively charged free electrons. Question 1: What is the source of this positive charge? Question 2: How does this current help determine the ionization threshold potential?

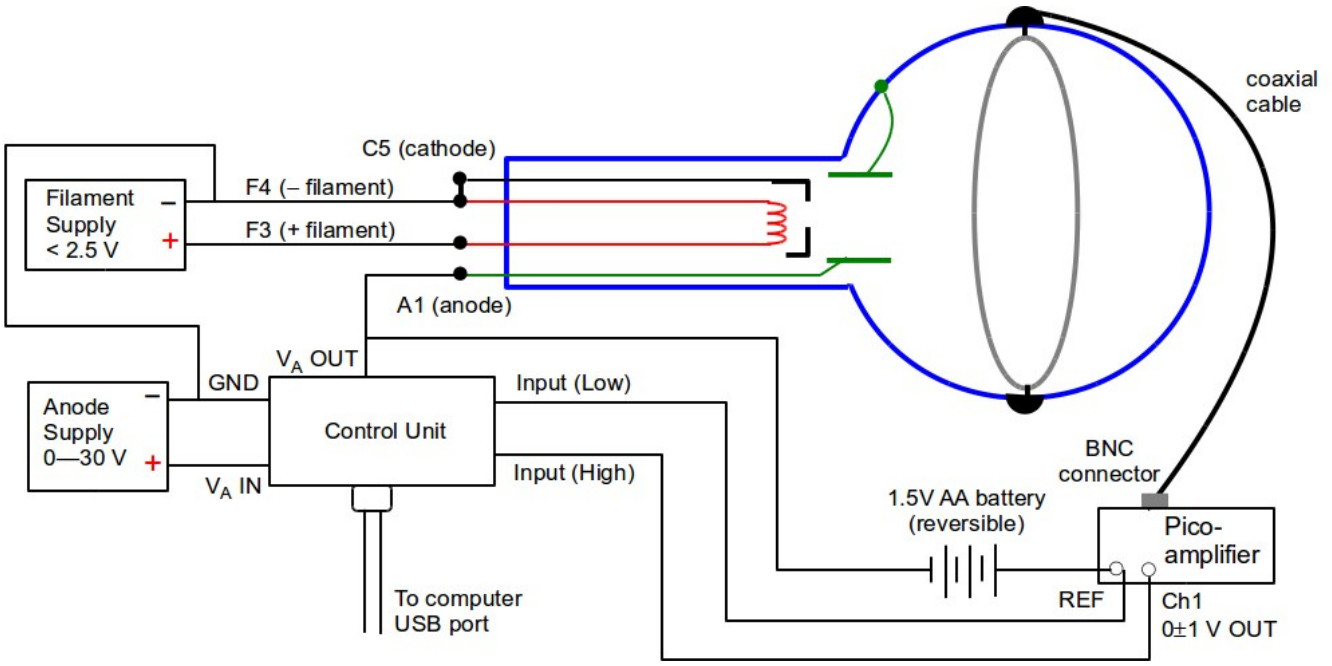

Fig. 1 Franck-Hertz experiment with helium gas

The DAQ device in the control unit reads a voltage at the pico-amplifier output that is directly proportional to the detector current. Connect the amplifier output to the control unit inputs as shown. The reference potential of the pico-amplifier (REF) must be allowed to float with respect to circuit ground (GND). Do not connect GND to REF. This is a differential measurement so the polarity only affects the sign of the signal. Turn on the filament supply (< 2.5V) and let it warm up for about a minute. Turn on the anode supply and set the voltage (V_A IN) to 3—4 V higher than the maximum anode voltage that will be applied (V_A OUT). Observe the proper polarity and never exceed 50V, otherwise the control unit will be damaged.

Open the LabView program named scan.vi. The program will instruct the control unit to quickly scan the anode voltage across a specified range and record a voltage corresponding to current in the collector ring electrode. The user must enter a starting and ending anode voltage as well as the voltage increment. The increment is the voltage step between successive data points. The finer the increment, the more data points will be taken.

It is important to understand that analog and digital instruments are not infinitely precise. The DAQ controller is a digital device with 10-bit resolution on its control voltage. This means its output voltage can be written with a precision of one part in 2^{10} or about 0.1%. As a result, the anode voltage cannot be specified to better than about 80 mV. It makes no sense to have a voltage increment smaller than this because it exceeds the resolution of the DAQ device.

Orient the 1.5V bias battery as shown in the above figure. Plug in the power supply of the pico-amplifier and set it for maximum gain by sliding the selector switch to the level marked 10^{-12}. It is a good idea to begin with a coarse scan over a range of 10—25V (not critical) to verify proper setup of the experiment. Press the run button (horizontal arrow) on the LabView front panel to start the program. The goal is to identify four peaks corresponding to energy levels 2^3S, 2^1S, 3^1S,

and 4^1S (overlaps with 4^3S) in helium.

The detected voltage is directly proportional to the current in the ring electrode. The control unit reads it using an 11-bit A-D (analog-to-digital) converter. Its resolution accuracy is a factor of 2 better than the anode voltage controller. The sensitivity of the input A-D converter can be adjusted on the LabView interface. Highest accuracy is attained when the converter is set for the minimum voltage level that does not cause saturation, i.e. when the input voltage exceeds the selected sensitivity. Example: If the maximum absolute detected voltage from the scan is slightly higher than 1V, set the input sensitivity to 1.25V. The pico-amplifier will clip any voltage greater than about 4V. If this occurs, reduce the gain to 10^{-11}. When you have the desired data, save it to disk. The data is written as a two-column spreadsheet.

You should be able to identify four peaks before ionization of the gas commences. The ionization threshold is characterized by an abrupt increase of the slope of absolute current with anode voltage. Note: The collected current is very small and can be disturbed by potentials from objects outside of the glass tube (eg. the experimenter's body). Repeat the experiment at a higher or lower filament voltage, making sure not to exceed 2.5V. Comment on any differences in the shape of the emission spectra; the peaks should be seen at the same anode voltages.

Reverse the 1.5V battery to collect positive charge and repeat the scan. The experiment is much less sensitive to resonant excitation of the atoms, but one can expect an increase of the current slope in the vicinity of the ionization potential, i.e. the inflection point of the curve defines the ionization threshold. The anode voltage does not need to exceed 30V.

At this point, sufficient data has been collected to complete the Objectives of Part 1.2.

Troubleshooting

- If the LabView program cannot communicate with the DAQ device (Measurement Computing 1208LS), check that the USB interface cable is properly connected. Open the installed program InstaCal, verify that the device is recognized, and attempt to communicate with it. Check that it is configured with 4 inputs in differential mode.

- If the LabView program cannot reach the specified maximum voltage, check that the anode power supply is properly connected to the control unit. If this is correct, either the power supply voltage must be increased or the upper limit scan voltage reduced.

- Absence of a detector current may indicate that the pico-amplifier is off or the glass bulb is not fully pressed into its socket.

Part 2: Excitation of mercury

2.1 Equipment

Triode tube filled with mercury (Manufactured by Neva)
AC heater cord
Thermometer
0096 Control unit

Pico-amplifier (Note: the detachable digital ammeter display is not used)
Filament power supply (6V at ~ 0.3 A)
Anode power supply (0—50V)
1.5V battery
PC with LabView program
Digital multimeter

The mercury tube replaces the helium bulb. The 0096 control unit and LabView program from Part 1 are used.

2.2 Objectives

1) Identify the first excited state of mercury in units of *eV*. Compare to the established value.
2) Study the effect temperature, while keeping it below 200C.
3) Determine the work function of the oxide coated cathode.

2.3 Procedure

The tube must be uniformly heated to a temperature in the range 150—200C to produce mercury vapor. This is accomplished with a 400W heating element inside the enclosure. AC power is applied to the heater using the 2-pin connection on the lower left side panel. Insert the thermometer about halfway into the box at the access hole on the top. A clip holds it in place. Turn on the heater AC power switch and set the temperature using the thermostat control dial on the right side panel. An initial dial setting of about 6—7 should be adequate. Allow about 15 minutes for the temperature to stabilize. Do not exceed 200C.

Caution: The enclosure will get hot enough to cause skin burns. Take proper safety precautions.

Make the electrical connections as shown in the schematic diagram below, using a shielded BNC cable between the collecting electrode and amplifier. The filament power supply should provide 300 mA of current at 6V. Wait 90 seconds for it to heat the oxide-coated cathode (K).

Take data in the same way as the helium experiment in Part 1. Set the anode supply voltage (V_A IN) to 3—4 V higher than the maximum anode voltage that will be applied (V_A OUT). Observe the proper polarity and never exceed 50V, otherwise the control unit will be damaged. In addition, the reference potential of the pico-amplifier (REF) must be allowed to float with respect to circuit ground (GND). Do not connect GND to REF.

The helium experiment measures a secondary current from scattered electrons such that resonances occur at current peaks. In the mercury setup, *minima* in the plot of collector current vs anode voltage identify the quantum energy excitations. The collector electrode (M) monitors current due to electrons passing directly through the mesh anode (A). Different pico-amplifier and DAQ settings in the LabView program will also be needed to get clean data. The 1.5V battery provides a decelerating potential to slow electrons before they strike the collector. Electrons that have lost most of their energy through inelastic collisions cannot overcome this potential.

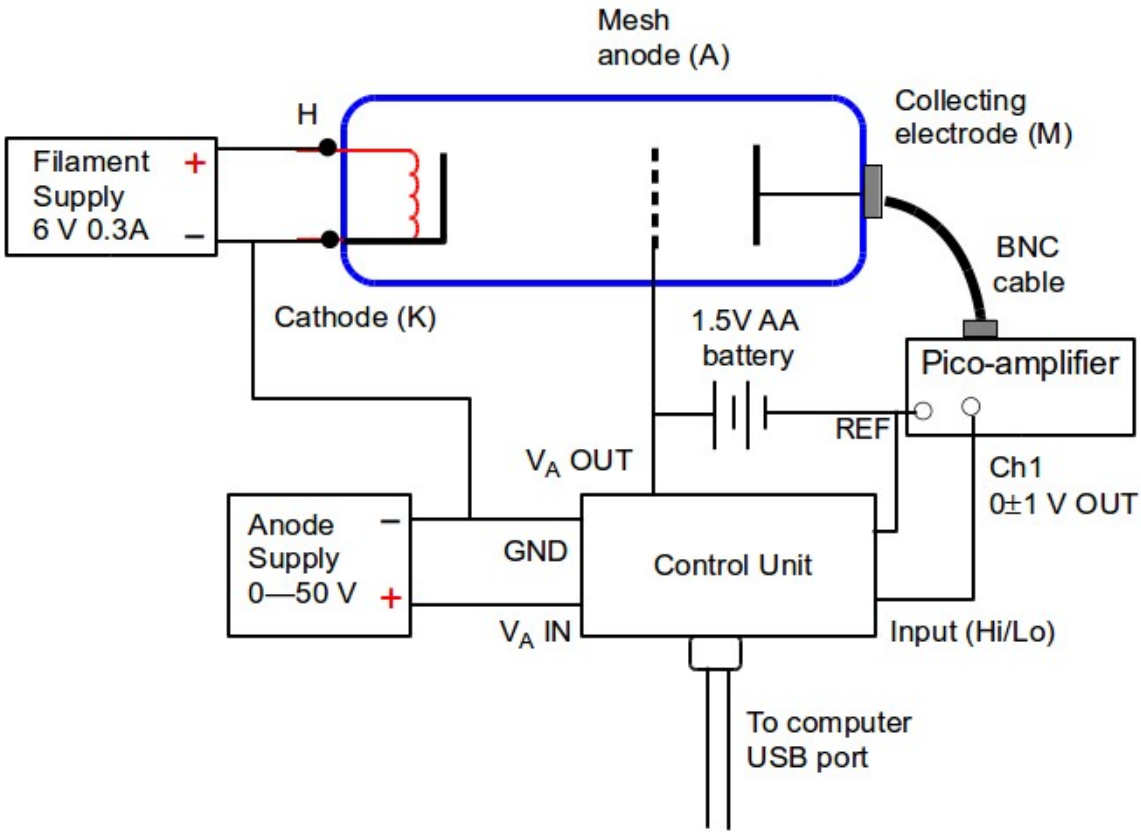

Fig. 2 Franck-Hertz experiment for mercury vapor

When configured correctly, the collected current data will show a sequence of peaks and valleys with increasing anode voltage. The voltage separation of the valleys should be nearly identical and correspond to the excitation energy of a mercury atom. Away from resonance, collisions are purely elastic – no energy is transferred to the mercury atoms. Near the resonant energy, electrons will lose a quantum of energy via inelastic collisions causing the current to drop dramatically. At higher anode voltage, elastic collisions resume and current goes back up. Increasing the voltage further will again lead to inelastic collisions from resonant excitation. This secondary excitation region moves away from the mesh anode, closer to the cathode. The electron has enough energy remaining after its first inelastic collision to excite a second atom on its way to the anode. With more voltage the electron can excite a third atom, then a fourth and so on, as it traverses the path to the anode. This is the cause of the observed integer-multiple sequence.

Note that the absolute value of the first valley will have a positive offset due to the work function of the cathode. Report this value. (This offset was not relevant in the helium experiment) Using the collected data, determine the resonant excitation energy of mercury atoms. Perform a statistical analysis of your data set and interpret the results. What are the sources of measurement uncertainty? What is the total uncertainty of your measurement?

The characteristics of the plot are affected by temperature. Obtain data at 150C and a higher temperature around 190C (do not exceed 200C). Describe the differences. Note: If the temperature in the enclosure is too low and the anode voltage set too high, breakdown in the tube may take place. The tube has an internal resistor to protect it from breakdown, but this condition should be avoided.

Energy levels in helium and neon atoms by an electron-impact method

N. Taylor, K. D. Bartle, and D. Mills
Department of Physical Chemistry, University of Leeds, Leeds LS2 9JT, England

D. S. Beard
Teltron Limited, 32/36 Telford Way, London W3, England
(Received 7 February 1980; accepted 20 May 1980)

Electronic energy levels in noble gas atoms may be determined with a simple teaching apparatus incorporating a resonance potentials tube in which the electron beam intensity is held constant. The resulting spectra are little inferior to those obtained by more elaborate electron-impact methods and complement optical emission spectra. Singlet–triplet energy differences may be resolved, and the spectra of helium and neon may be used to illustrate the applicability of Russell–Saunders and other, "intermediate," coupling schemes.

I. INTRODUCTION

Determination of the ionization potentials of rare gases using commercial gas-filled thermionic tubes[1] is a familiar experiment in many teaching laboratories. However, the characteristics of certain of these are often difficult to interpret and in any case seldom yield information about electronically excited states before ionization. In this article we describe an electron-impact method using a resonance potentials tube which, with an associated voltage-scanning and emission-stabilizing unit, enables both ionization potentials and the energies of various electronic levels to be determined. The experiment thus complements conventional studies of emission spectra by spectroscopic methods since the optical selection rules are now relaxed. The results obtained compare favorably with those from more advanced methods such as the use of sulphur hexafluoride to scavenge the low-energy electrons or high-resolution electron-energy-loss spectrometry.

II. ELECTRON IMPACT METHOD USING RESONANCE POTENTIALS TUBES

The construction of the resonance potentials tube[2] is shown schematically in Fig. 1. The simple diode electron gun is contained in a sidearm and allows electrons at a kinetic energy determined by the anode potential to be passed as a divergent beam across the cell containing a gas at low pressure to be collected at a conducting coating held at the same potential as the anode. A ring electrode within the cell is positioned so as to avoid collection directly from the incident beam, but when biased with a small positive potential (1.5 V) with respect to the anode the ring can collect electrons which have imparted most of their energy to gas atoms on impact. The enhanced sensitivity to electrons of low energy gives large ring electrode currents only when the energy of the incident beam matches that of an electronic transition in the gas atoms, and a spectrum of *resonance* or *critical* potentials is thus obtained on scanning a range of anode potential. In this mode the approach to ionization is indicated by a progressively increasing ring current with anode potential as many more transitions become possible. Reverting to a small negative ring potential enables ionization to be observed more directly from the onset of ion collection.

The control unit carries out the following functions:

(a) The electron beam intensity is maintained at a constant level irrespective of anode potential. This emission stabilization is important in obtaining good resolution from the commercially available tubes.

(b) The anode potential may be "ramped" as a linear variation with time within the range 10–30 V or may be adjusted to hold at some fixed value.

(c) The ring electrode currents are monitored with a simple solid state electrometer and the output used to drive a potentiometric recorder.

A circuit diagram is available on request from the authors.

III. OPTICAL SPECTRA AND SELECTION RULES

The spectra of most small and medium size atoms are in accord with Russell–Saunders LS coupling in which the electrostatic interactions are dominant over spin-orbit terms in determining the major separations of the energy levels. L and S are "good" quantum numbers at this extreme and term symbols generated from the various values of L and S serve as a simple and convenient way of identifying the energy levels and hence the spectral lines. The selection rules now include $\Delta L = 0, \pm 1$ ($L = L' = 0$ not allowed) and $\Delta S = 0$ to supplement the more general cases $\Delta J = 0, \pm 1$ ($J = J' = 0$ not allowed) and $\Delta l = \pm 1$ (the Laporte rule) which forbids transitions between states of the same "parity," i.e., either both even (Σl_i = even integer) or both odd (Σl_i = odd integer). When spin (own) orbit coupling is small, secondary splitting arises according to a given pattern which depends on atomic number Z. For $Z \leq 4$ the split levels have decreasing energy with increasing J and for $Z > 4$ the order tends more and more to be reversed. One outcome is the Landé interval rule, which states that the energy interval between pairs of adjacent levels is proportional to the J value of the upper level of each pair, but deviations from this occur because of neglect of spin-other-orbit and spin–spin magnetic interactions. Helium gives one of many possible examples of the characteristic energy level pattern determined by LS coupling (see Table I); the fine splitting of the 2^3P states, for example, due to the magnetic terms are in this case less than 1 cm^{-1} and are not in accord with the interval rule.

 0002-9505/81/030265-04$00.50

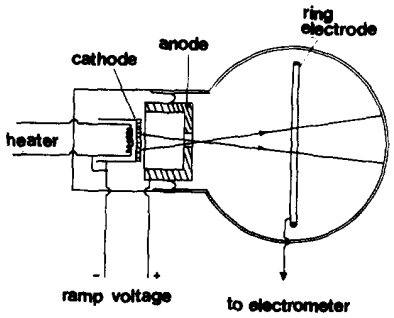

Fig. 1. Resonance-potentials tube.

Although often used, LS term symbols for atoms in which the electron interactions are grossly distorted from those described above have more limited usefulness in that levels have major separations due to other than electrostatic terms and the sense of "order" can be lost. In addition, selection rules, intensity relationships, etc. derived at the LS extreme are not now applicable. Two major factors disturb LS coupling as a useful representation. For "not too highly excited states" the spin (with own) orbit energies increase more rapidly with atomic number Z than the electrostatic terms such that they are dominant at high Z. At this situation the interaction energy depends primarily on the spin-orbit terms of the "core" of unexcited electrons and somewhat less so on the spin-orbit term of the excited or "optical" electron. This $J_c j_2$ or $j_1 j_2$ coupling,[3] when pure, thus neglects the electrostatic terms between the core and optical electron that at the LS extreme contributed to the separation of the levels. The levels thus appear for a given configuration as two widely spaced pairs and in, say, a p^5np configuration where J_c and j_2 can both take values of $\frac{3}{2}$ and $\frac{1}{2}$ have designations $\{\frac{3}{2}, \frac{1}{2}\}$ $(J = 1,2)$, $\{\frac{3}{2}, \frac{3}{2}\}$ $(J = 0,1,2,3)$, (widely separated from) $\{\frac{1}{2}, \frac{1}{2}\}$ $(J = 0,1)$ and $\{\frac{1}{2}, \frac{3}{2}\}$ $(J = 1,2)$ in order of ascending energy. J_c and j_2 (at this limit) are "good" quantum numbers and selection rules now include $\Delta j_2 = 0, \pm 1$ ($j_2 = j_2' = 0$ not allowed) and $\Delta J_c = 0$. The second feature disturbing LS coupling occurs when excitation is large. In this case the spin-orbit term of the optical electron diminishes most rapidly with increasing n and thus can become negligible compared with the coupling of the orbital angular momenta of optical electron and core. The combinations of J_c and l_2 (optical electron) yield a good quantum number K, and levels thus appear as closely spaced pairs dependent on S_2 for the final splitting. This form of pair coupling has wide applicability and is termed $J_c l_2$, or occasionally jK, coupling. Among the heavier rare gases the $2p^5 3p$ configuration of neon involves relatively large electrostatic but small spin-orbit terms and thus follows the general pattern of LS coupling whereas $2p^5 4p$, $5p$, $6p$ configurations, etc. are more akin to the $J_c l_2$ pair coupling scheme.[4] Likewise as Z increases, pair coupling becomes more suitable for all configurations. The selection of a suitable term representation for a given case is best determined by a comparison of the calculated relative splittings in a given configuration with those experimentally determined. Here the relative contributions of the various electron interaction terms are assessed within some framework of approximations. The most suitable type of term symbol is that reflecting most closely those conditions. Likewise, relative line intensities, g factors, etc. may be compared with experimentally determined values to confirm the scheme. Using this approach Cowan and Andrew[5] suggest for the $2p^5 3p$ configuration of neon that a scheme based on Ls coupling is perhaps most applicable. In this further example of pair coupling the ll interactions are dominant, with the spin-orbit term of the core the other major contribution. Despite this, $J_c l_2$ representations are most commonly used for neon and many other atoms and we shall follow this convention in the discussion of our results and in Table II.

Selection rules for transitions caused by electron impact are expected to differ greatly from those applicable to interaction with photons since the incident electron has spin thus relaxing spin conservation ($\Delta S = 0$); the parity restrictions are also relaxed since these are applicable only when electric dipole radiation is involved. Essentially we shall determine the significance of such changes from a comparison with the optical spectra.

IV. RESULTS AND DISCUSSION

Helium

Figure 2 [curve (a)] illustrates a typical recorder trace of resonance potentials for a tube filled with helium; curve (b) is the corresponding current due to He^+ ion collection when the ring electrode is biased negatively. The voltage axis in these cases has been "corrected" by assuming the literature value[6] of 24.58 V for the first ionization potential. The resonance potentials correspond to transitions from the ground state 1^1S to the levels indicated. These energies may be compared with values obtained spectroscopically (Table I).

Although the precision is lower, the technique gives results comparable with optical methods. However, the observations of transitions from the ground state and of the many optically forbidden transitions are particularly useful additions to the complementary optical procedure. Thus we

Table I. Energy levels and resonance potentials of helium. Transition to levels marked * from the ground state are forbidden by optical selection rules.[a]

Observed resonance potentials		Electron energy levels from optical spectroscopy LS		
(eV)	(cm^{-1})	term symbol	(eV)	(cm^{-1})
19.85	160000	$*2^3S_1$	19.819	159850
20.70	167000	$*2^1S_0$	20.615	166270
		$*2^3P_{2,1,0}$	20.963	169080
		2^1P_1	21.218	171130
22.90	185000	$*3^3S_1$	22.718	183230
		$*3^1S_0$	22.300	184860
		$*3^3P_{2,1,0}$	23.007	185560
		$*3^3D_{3,2,1}$	23.074	186100
		$*3^1D_2$	23.074	186100
		3^1P_1	23.086	186200
23.70	191000	$*4^3S_1$	23.593	190290
		$*4^1S_0$	23.672	190930
		+ other $n = 4$ levels		

[a]Data mainly taken from A. R. Striganov and N. S. Sventitskii, *Tables of Spectral Lines of Neutral and Ionized Atoms* (Plenum, New York, 1968).

Table II. Energy levels and resonance potentials of neon. Transition to levels marked * from the ground state are forbidden by optical selection rules.[a]

Observed resonance potentials		Electron energy levels from optical spectroscopy designation			
(eV)	(cm^{-1})	LS	$J_c l_2$	(eV)	(cm^{-1})
16.70	134500		$*3s[1\frac{1}{2}]^0_2$	16.615	134040
			$3s[1\frac{1}{2}]^0_1$	16.671	134460
			$*3s'[\frac{1}{2}]^0_0$	16.716	134820
			$3s'[\frac{1}{2}]^0_1$	16.849	135890
18.65	150500	$^3S_1$	$*3p[\frac{1}{2}]_1$	18.38	148260
		$^3D_3$	$*3p[2\frac{1}{2}]_3$	18.555	149660
		$^3D_2$	$*3p[2\frac{1}{2}]_2$	18.57	149830
		$^3D_1$	$*3p[1\frac{1}{2}]_1$	18.61	150120
		$^1D_2$	$*3p[1\frac{1}{2}]_2$	18.64	150320
		$^1P_1$	$*3p'[1\frac{1}{2}]_1$	18.69	150770
		$^3P_2$	$*3p'[1\frac{1}{2}]_2$	18.70	150860
		$^3P_0$	$*3p[\frac{1}{2}]_0$	18.71	150920
		$^3P_1$	$*3p'[\frac{1}{2}]_1$	18.73	151040
		$^1S_0$	$*3p'[\frac{1}{2}]_0$	18.966	152970
19.75	159500		$*4s[1\frac{1}{2}]^0_2$	19.66	158600
			$4s[1\frac{1}{2}]^0_1$	19.689	158800
			$*4s'[\frac{1}{2}]^0_0$	19.76	159380
			$4s'[\frac{1}{2}]^0_1$	19.780	159540
20.10	162000		$*3d[\frac{1}{2}]^0_0$	20.020	161510
			$3d[\frac{1}{2}]^0_1$	20.027	161530
			$*3d[3\frac{1}{2}]^0_4$	20.034	161590
			$*3d[3\frac{1}{2}]^0_3$	20.034	161590
			$*3d[1\frac{1}{2}]^0_2$	20.037	161610
			$3d[1\frac{1}{2}]^0_1$	20.041	161640
			$*3d[2\frac{1}{2}]^0_2$	20.048	161700
			$*3d[2\frac{1}{2}]^0_3$	20.048	161700
			$*3d'[2\frac{1}{2}]^0_2$	20.136	162410
			$*3d'[2\frac{1}{2}]^0_3$	20.136	162410
			$*3d'[1\frac{1}{2}]^0_2$	20.115	162420
			$3d'[1\frac{1}{2}]^0_1$	20.140	162440
			$5s[1\frac{1}{2}]^0_1$	20.57	165907
Here selected levels only are listed			$6s[1\frac{1}{2}]^0_1$	20.95	168972
			$7s[1\frac{1}{2}]^1_1$	21.14	170504
			$8s[1\frac{1}{2}]^0_1$	21.26	171472

[a]Data mainly taken from A. R. Striganov and N. S. Sventitskii, *Tables of Spectral Lines of Neutral and Ionized Atoms* (Plenum, New York, 1968).

see transitions to 2^3S, 2^1S, and 2^3P—violating $\Delta S = 0$, $L = L' = 0$, and $\Delta S = 0$, respectively—and many other examples. Transitions to 3^1D and 3^3D are probably present ($\Delta J > 1$) although at lower intensity than for lower ΔJ values. Of particular interest is the direct observation of the 2^3S–2^1S energy difference with its implications in terms of the pairing energy of electrons.

Spectra obtained with this simple teaching apparatus are not too inferior to those observed with more elaborate electron impact methods. In curve (c) of Fig. 2 we reproduce results similar to those obtained by Brion and Olsen[7] in which SF_6, which has a high electron-capture cross section only for energies <0.02eV, is used to "scavenge" the low-energy electrons; the concentration of SF_6^- ions is measured in a negative-ion mass spectrometer. The performance of the resonance potentials tube when detecting He^+ ions is clearly far superior to methods using "electron tubes," due in part to emission stabilization.

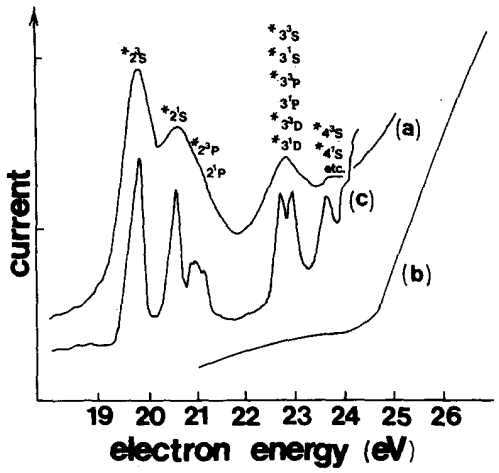

Fig. 2. Electron-impact spectra of helium: (a) this work; (b) He^+ current; (c) electron impact with SF_6 scavenging (after Brion and Olsen[7]).

Neon

In Fig. 3 we compare our resonance potentials (a) with those obtained using SF_6 scavenging (b) and high-resolution electron-energy-loss spectrometry (c).[8] The neon resonance potentials tube performs very well and results are quite similar to those obtained using the more complicated scavenging technique.[7] We have included curve (c) to enable some prediction to be made of the relative contributions of various transitions. In Table II we list a selection of energy levels for the neon atom and the corresponding resonance potentials we observe. The designations are generally in $J_c l_2$ notation and are of the form $nl'[K]^\circ_J$ where the l value of the optical electron is "dashed" only when $J_c = \frac{1}{2}$, otherwise $J_c = \frac{3}{2}$. The superscript ° recognizes odd parity, and its absence even parity. In addition LS term symbols are given for the $2p^5 3p$ configuration for reasons mentioned in Sec. III. We see the strong contributions of transitions from the ground state to the parity-forbidden $2p^5 3p$ configuration and most likely similar contributions to higher-p states. Examination of the LS term symbols for this group indicates more simply the presence of transitions forbidden by the $\Delta S = 0$ selection rule. The $^3P_{2,1,0}$ states are degenerate at the LS extreme as also are $^3D_{3,2,1}$ and we see ac-

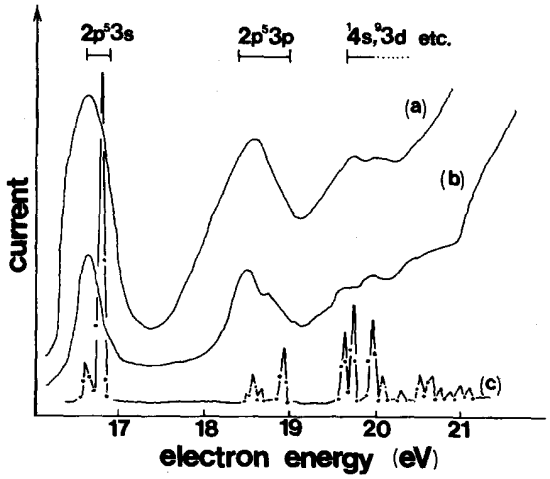

Fig. 3. Electron-impact spectra of neon: (a) this work; (b) with SF_6 scavenging (after Brion and Olsen[7]); (c) high-resolution trapped-electron excitation (after Roy and Carette[8]).

cording to Cowan and Andrew[5] the effects of predominantly core spin-orbit terms in splitting these levels. The peak at around 16.7 eV most probably involves predominantly the optically allowed transition from the ground state to $3s^2[1/2]_1^0$ but the detail of (c) indicates the presence of a contribution from all other states of the $2p3s$ configuration, thus including a $J = J' = 0$ and $\Delta J = 2$ transition. There are numerous other contributions which may be discussed in a similar way.

The neon tube may also be operated to collect Ne^+ ions. In this mode the performance in detecting the onset of ionization is again superior to methods using "electron tubes."

V. CONCLUSIONS

We have demonstrated that with relatively simple apparatus, resonance potentials tubes are capable of supplying interesting information concerning the energy levels of electrons in noble gases. In particular, emphasis can be placed on complementing emission spectra and on the operation of optical selection rules since many violations may be directly observed. In addition the implications of various coupling schemes in determining the patterns of levels for various configurations can be introduced to students. Finally, singlet–triplet energy differences can be resolved and serve as an interesting basis for a discussion of electron "pairing."

[1]R. B. Dineen and R. S. Nyholm, J. R. Inst. Chem. 110 (1963).

[2]A helium resonance potentials tube is available from Teltron Ltd., 32/36 Telford Way, London W3.

[3]It should be noted that because of the filled-shell ground state of the rare gases their behavior is formally similar to a two-electron system; despite this, the spin-orbit term of the "hole," for example, can greatly exceed that of the electron it "replaces." The term symbol for $J_c j_2$ coupling is presented here in the form $\{J_c, j_2\}$ $(J = \cdots)$.

[4]There are many excellent accounts of intermediate coupling, for example, E. U. Condon and G. H. Shortley, *The Theory of Atomic Spectra* (Cambridge University, Cambridge, 1935) and B. Edlen, *Handbuch der Physik, Vol. 27, Atomic Spectra* (Springer-Verlag, Berlin, 1964) provide additional discussion to that presented here.

[5]R. D. Cowan and K. L. Andrew, J. Opt. Soc. Am. **55**, 502 (1965).

[6]C. E. Moore, *Circular No. 467, Vol. 1* (National Bureau of Standards, Washington, D.C., 1949).

[7]C. E. Brion and L. A. R. Olsen, J. Phys. B **3**, 1020 (1970).

[8]D. Roy and J. D. Carette, Can. J. Phys. **52**, 1178 (1974).